Effect of ausforming on the bainitic transformation in medium carbon steels

Adriana Eres-Castellanos[1]

Tutor: Francisco Gálvez Diaz-Rubio[2]
Supervisors: Francisca G. Caballero[1] and Carlos Garcia-Mateo[1]

1 Department of Physical Metallurgy, National Center for Metallurgical Research (CENIM-CSIC)
2 Department of Materials Science, Technical University of Madrid (UPM)

Acknowledgements:

RFCS-2015-709607

Introduction: high strength steels (HSS)

- Recent years have seen the significant development of steels characterized by high strength (UTS>1500 MPa).
- It is expected that the HSS market value reaches 30.45 USD Billions by 2024.

M. M. Research, "Global High Strength Steel Market – Industry Analysis and Forecast (2017-2024) " 4178, 2017.

Introduction: nanostructured bainite

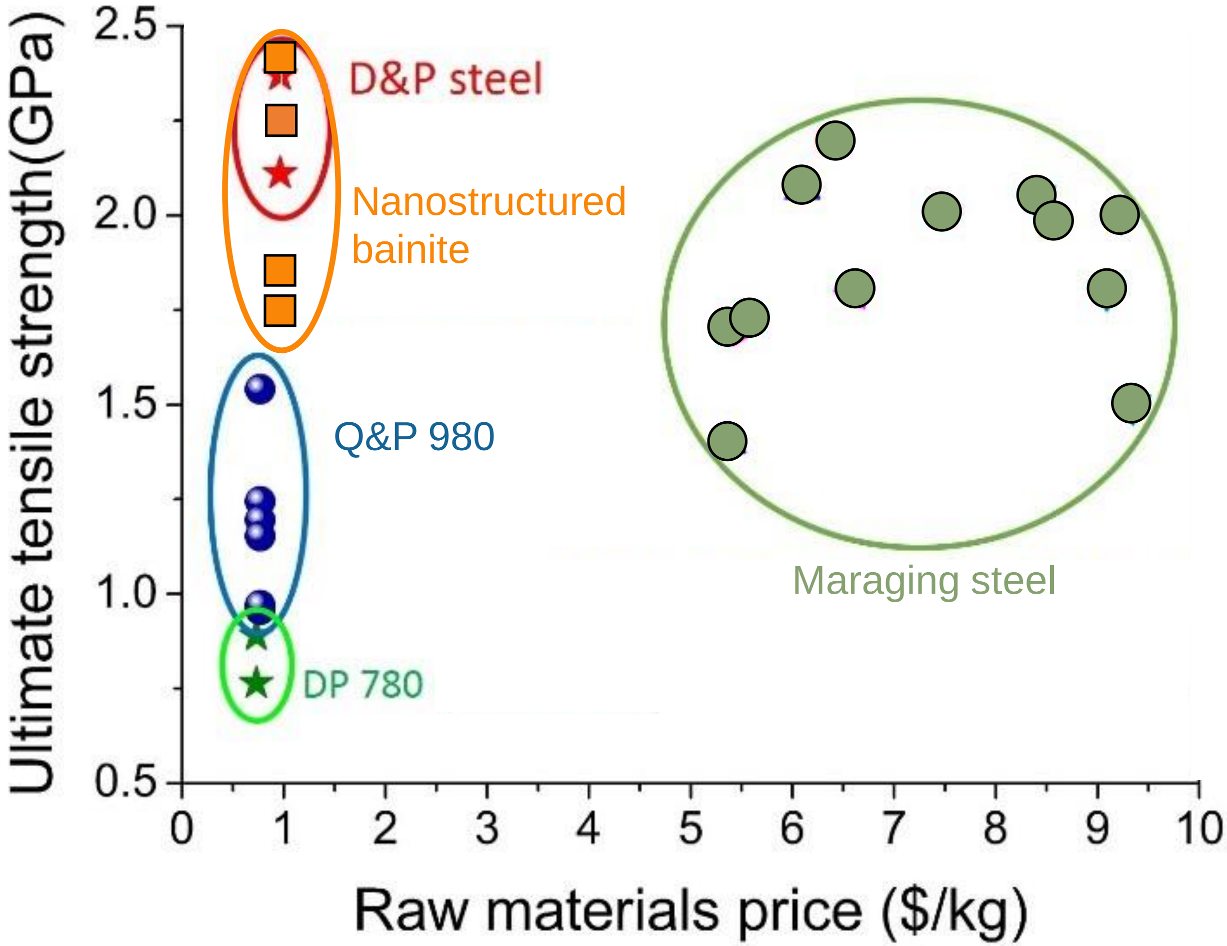

He, B. B., et al. "High dislocation density–induced large ductility in deformed and partitioned steels." Science 357.6355 (2017): 1029-1032.
Sun, Jun-jie, et al. "Super-strong dislocation-structured high-carbon martensite steel." Scientific reports 7.1 (2017): 6596.
Węglowski, M. S., J. Marcisz, and B. Garbarz. "Technological Properties and Applications of High-Carbon Nanobainitic Steels." Biuletyn Instytutu Spawalnictwa w Gliwicach 62 (2018).
Zhao, J., et al. "Extremely high strength achievement in medium-C nanobainite steel." *Scripta Materialia* 152 (2018): 20-23.

Introduction: nanostructured bainite

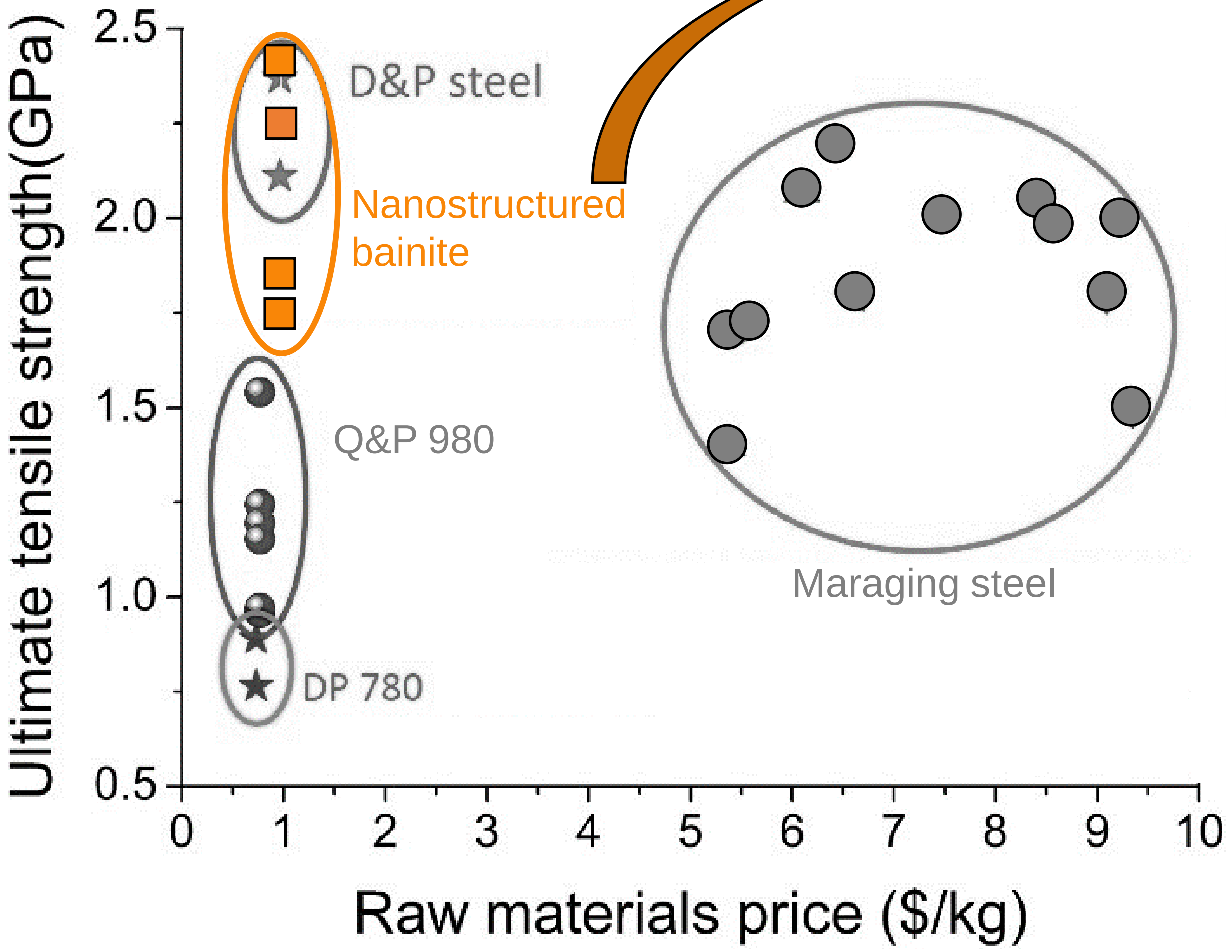

UTS = 1.8-2.2 GPa
TE up to 21 %
High wear resistance
High fatigue strength

He, B. B., et al. "High dislocation density–induced large ductility in deformed and partitioned steels." Science 357.6355 (2017): 1029-1032.
Sun, Jun-jie, et al. "Super-strong dislocation-structured high-carbon martensite steel." Scientific reports 7.1 (2017): 6596.
Węglowski, M. S., J. Marcisz, and B. Garbarz. "Technological Properties and Applications of High-Carbon Nanobainitic Steels." Biuletyn Instytutu Spawalnictwa w Gliwicach 62 (2018).
Zhao, J., et al. "Extremely high strength achievement in medium-C nanobainite steel." *Scripta Materialia* 152 (2018): 20-23.

Introduction: nanostructured bainite

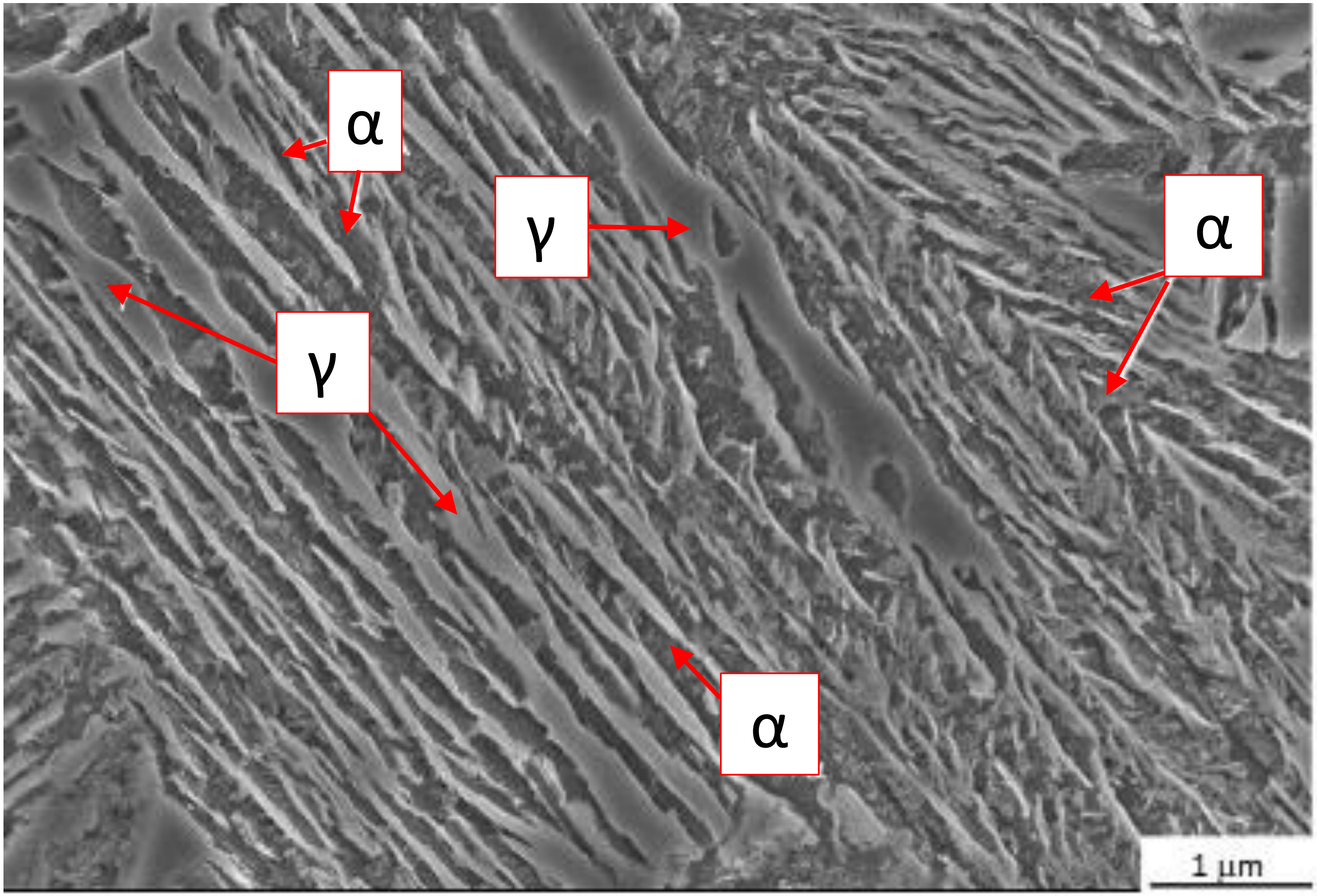

Garcia-Mateo, Carlos, et al. "Analyzing the scale of the bainitic ferrite plates by XRD, SEM and TEM." *Materials Characterization* 122 (2016): 83-89.

Introduction: nanostructured bainite

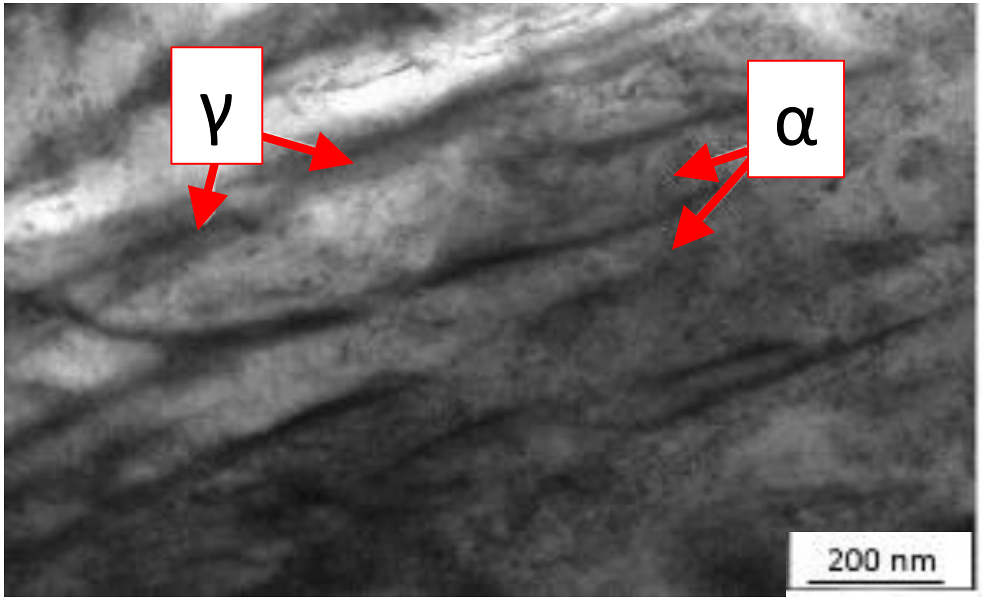

20 nm < α plate thickness < 100 nm

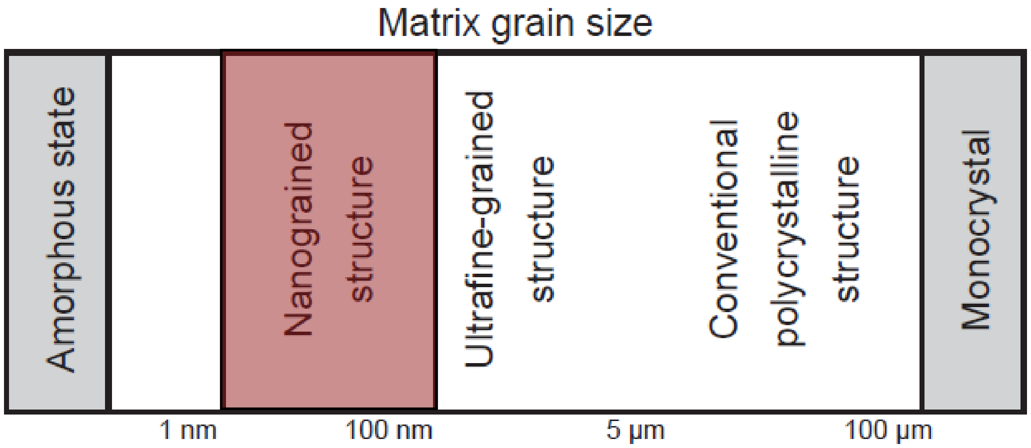

Garcia-Mateo, Carlos, et al. "Analyzing the scale of the bainitic ferrite plates by XRD, SEM and TEM." *Materials Characterization* 122 (2016): 83-89.
Węglowski, M. S., J. Marcisz, and B. Garbarz. "Technological Properties and Applications of High-Carbon Nanobainitic Steels." Biuletyn Instytutu Spawalnictwa w Gliwicach 62 (2018).

Introduction: nanostructured bainite

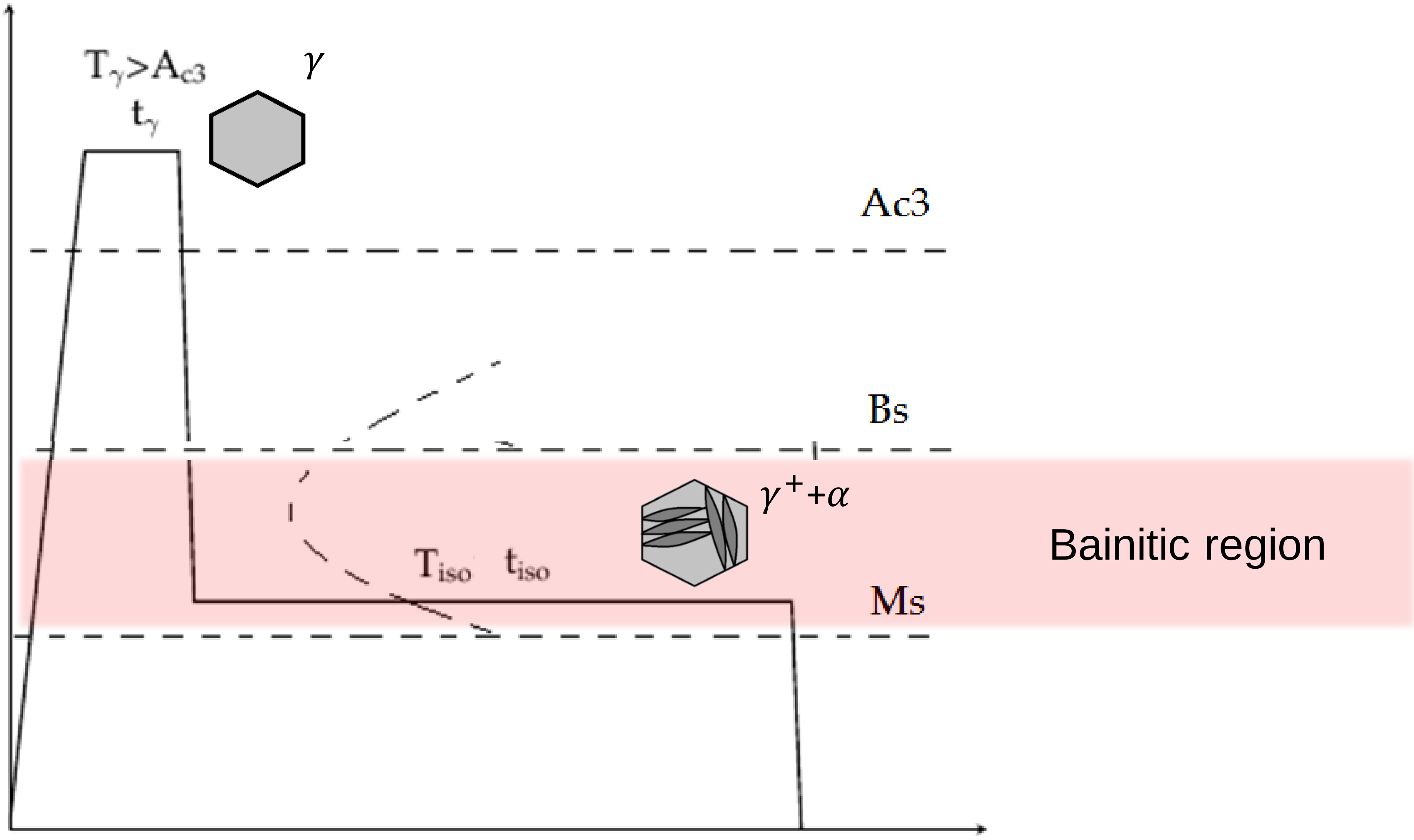

Introduction: nanostructured bainite

To obtain nanobainite, we need to transform from a stronger austenite. Typically:

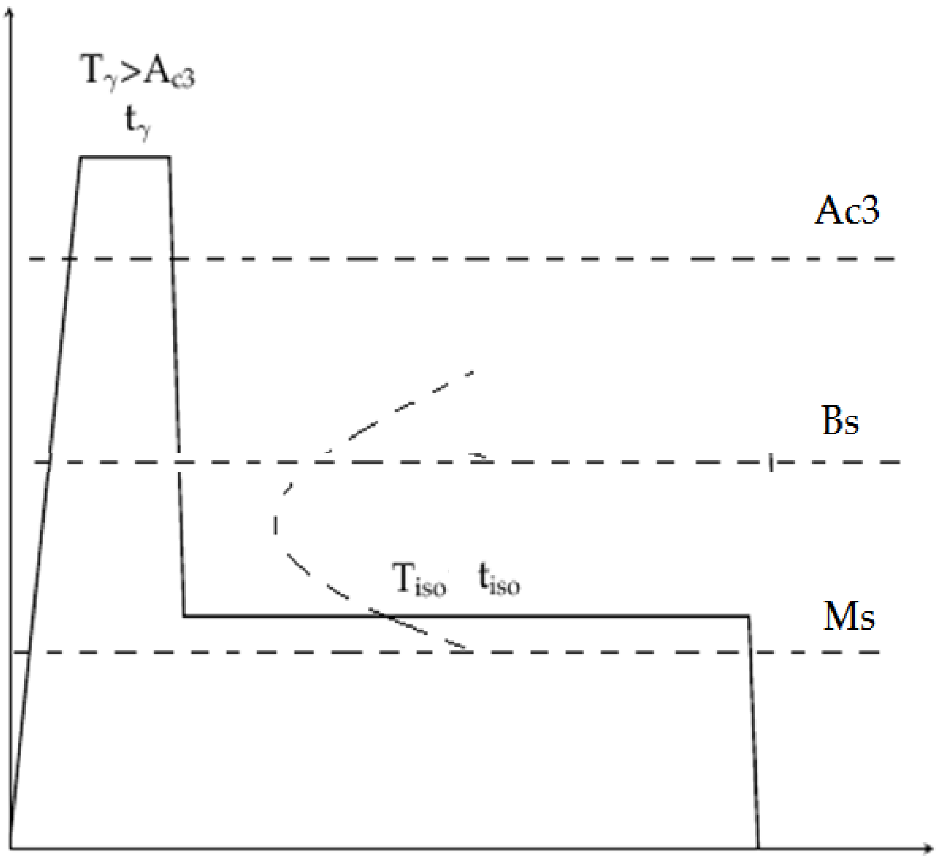

High carbon content (0.6-1 wt.%C)

↓

Low Ms and Bs

↓

Low T_{iso} (150-350 °C)

↓

Strong austenite

↓

Nanobainite

Introduction: nanostructured bainite

To obtain nanobainite, we need to transform from a stronger austenite. Typically:

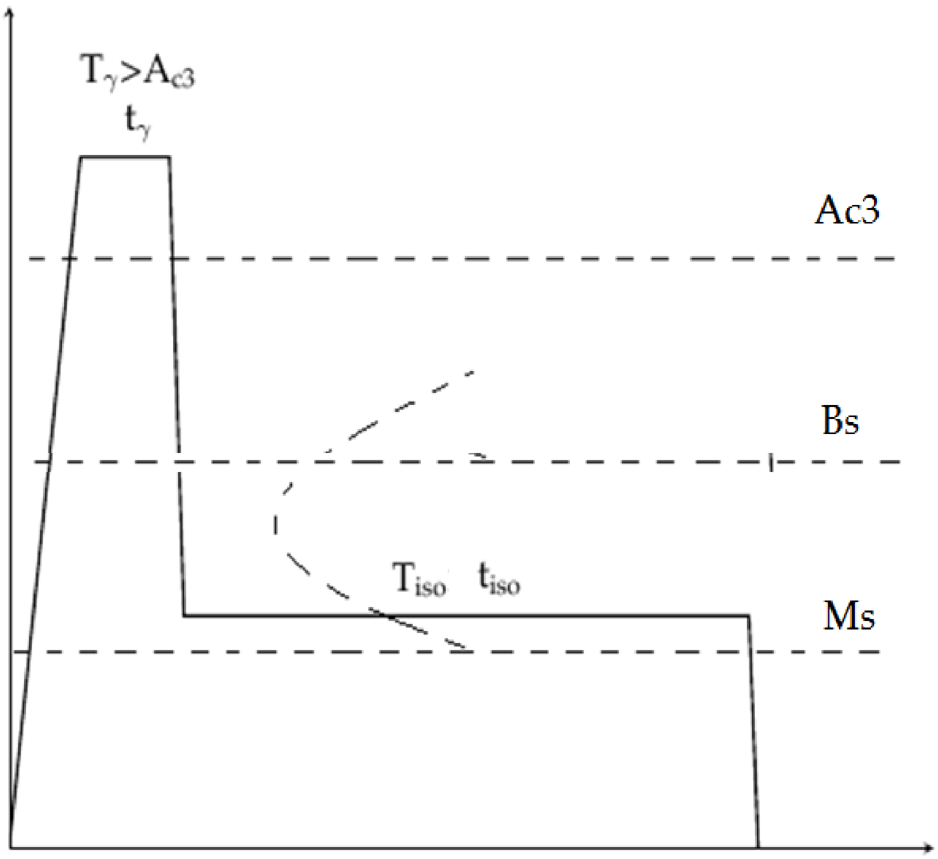

High carbon content (0.6-1 wt.%C)

↓

Low weldability / high hardenability

Long transformation times

Introduction: nanostructured bainite

To obtain nanobainite, we need to transform from a stronger austenite.
Alternatively, **ausforming**:

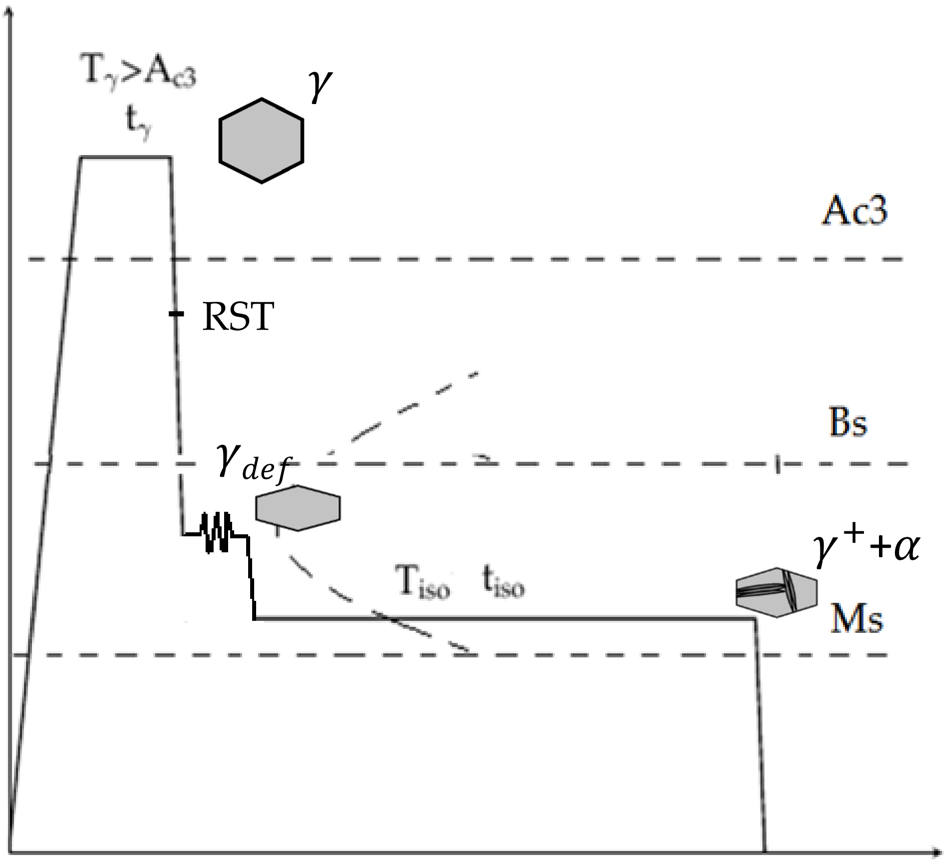

Austenite deformation below RST

↓

It is possible to decrease the steel carbon content
Strong austenite

↓

Nanobainite in lower carbon steels

↓

Better weldability / lower hardenability
Shorter transformation times

Materials and equipment

→Sidenor's commercial steel SCM40 (Fe-0.4C-3Si)

Materials and equipment

→Sidenor's commercial steel SCM40 (Fe-0.4C-3Si)

→ Dilatometer BÄHR 805 { fused silica push–rods (long. changes in length)
laser–interferometer (radial changes in length)

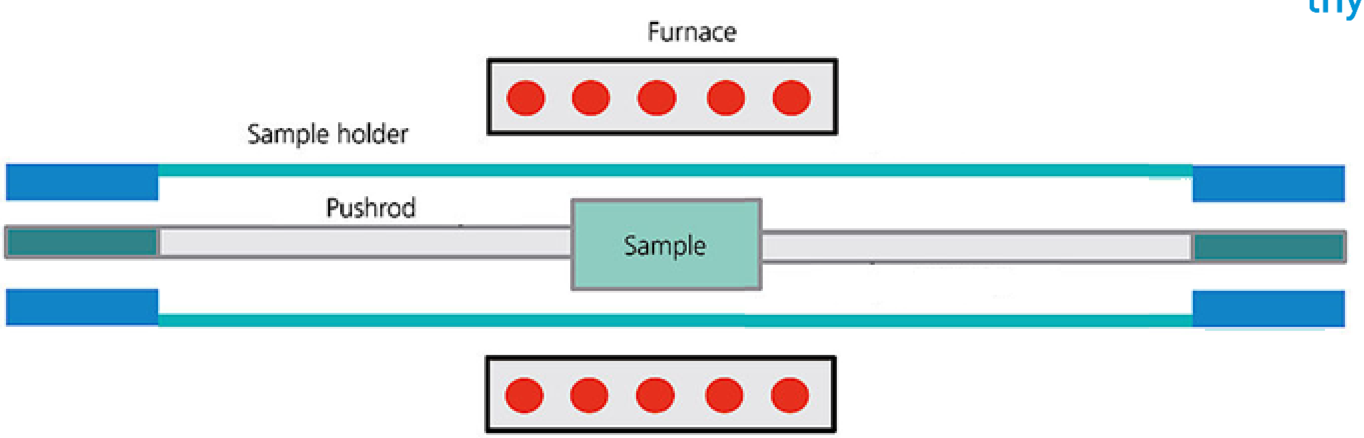

Materials and equipment

→Sidenor's commercial steel SCM40 (Fe-0.4C-3Si)

sidenor

→ Dilatometer BÄHR 805 {
- fused silica push–rods (long. changes in length)
- laser–interferometer (radial changes in length)
- silicon nitride punchers

thyssenkrupp

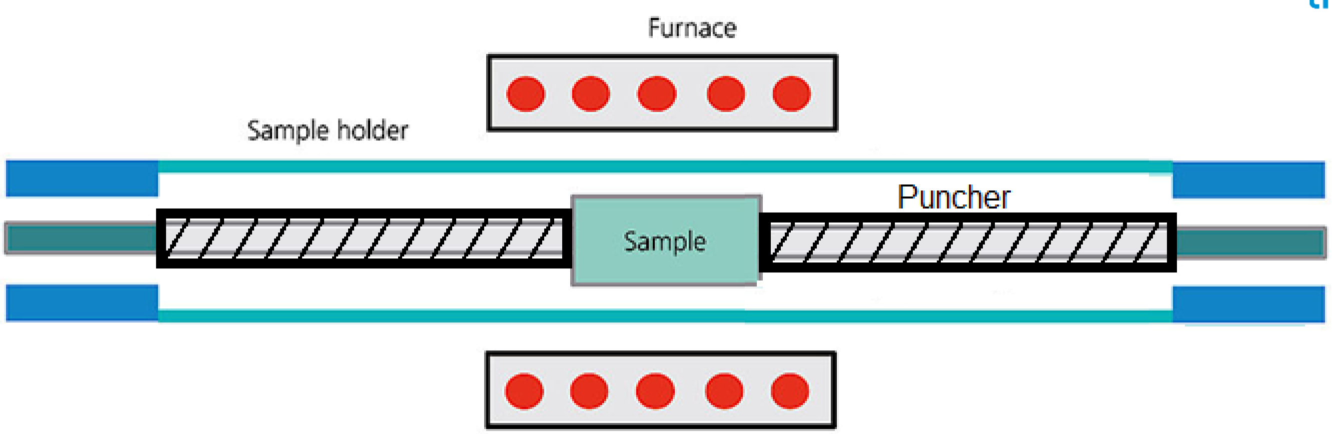

Materials and equipment

→Sidenor's commercial steel SCM40 (Fe-0.4C-3Si)

→ Dilatometer BÄHR 805 $\begin{cases} \text{fused silica push–rods (long. changes in length)} \\ \text{laser–interferometer (radial changes in length)} \\ \text{silicon nitride punchers} \end{cases}$

→JEOL JSM-6500 FEG-SEM

→Zeiss Auriga Compact FIB-SEM

→Matlab® (MTEX)

Thermal & thermomechanical treatments

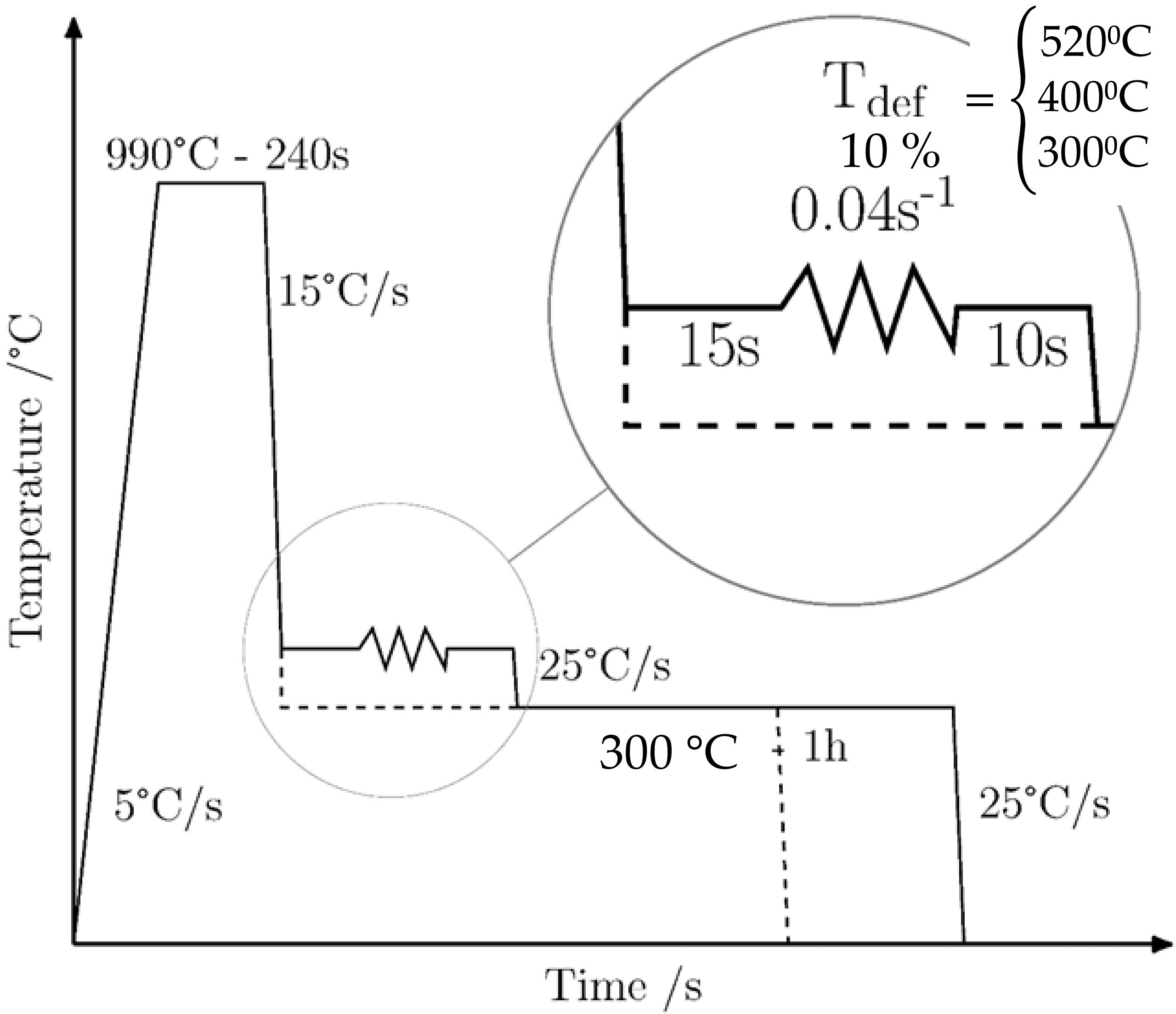

Thermal & thermomechanical treatments

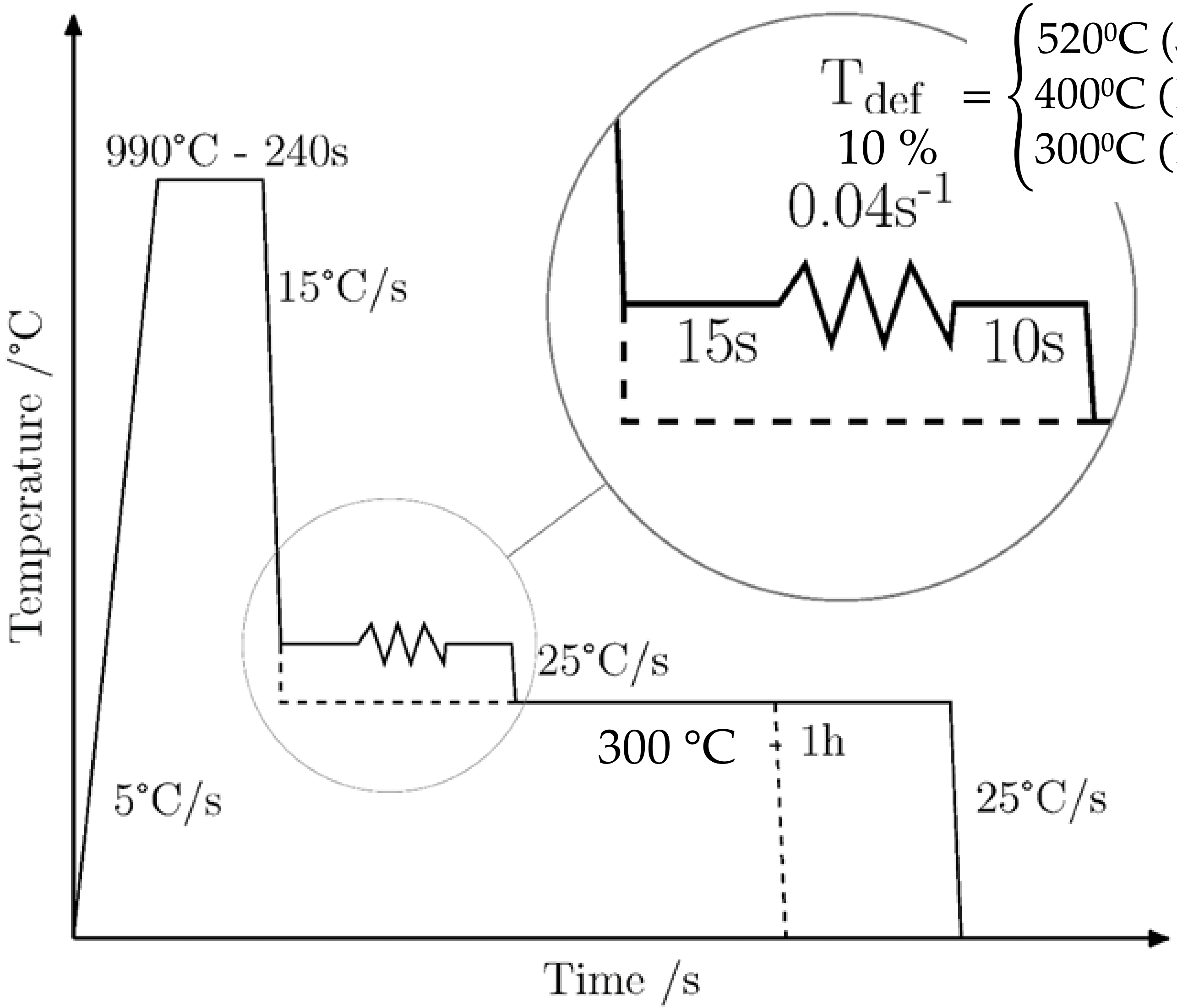

$T_{def} = \begin{cases} 520^0C\ (520\ ^0C > Bs \rightarrow MT) \\ 400^0C\ (Bs > 400\ ^0C > Ms \rightarrow LT) \\ 300^0C\ (Bs > 300\ ^0C > Ms \rightarrow LT) \end{cases}$

Results:
pure isothermal treatment at 300 °C

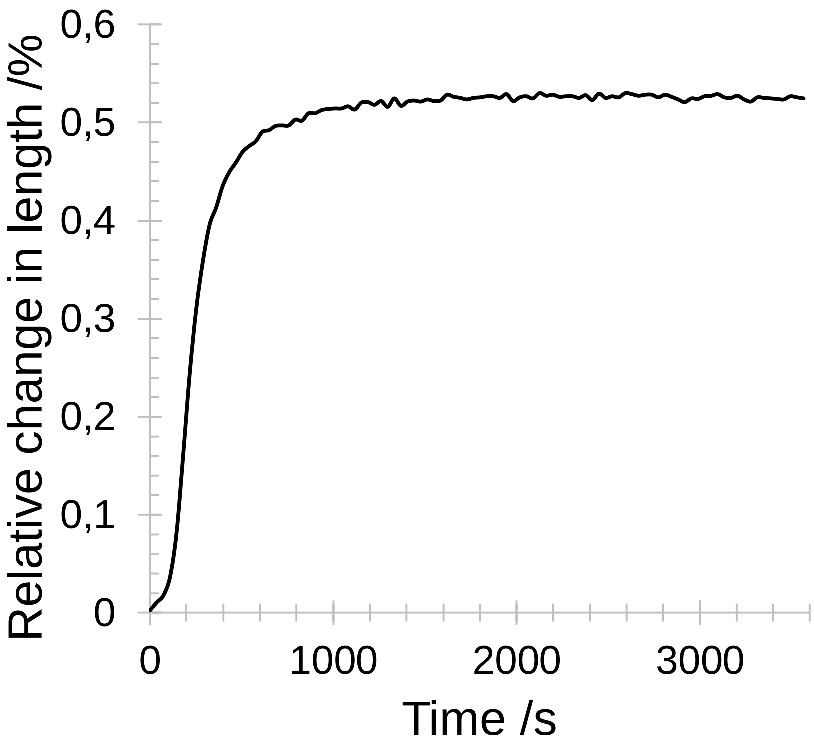

isotropic

Transverse section

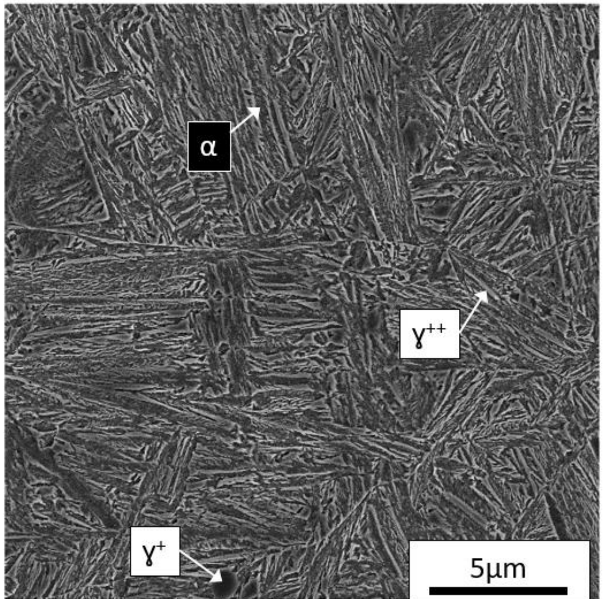

Longitudinal section

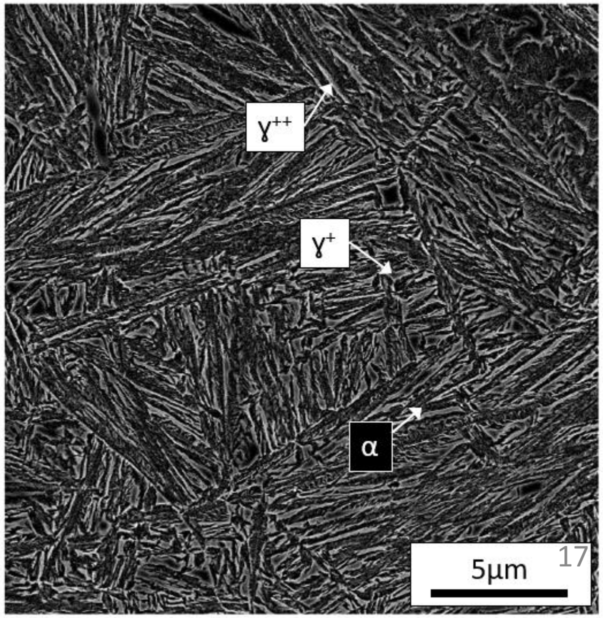

Results:

Ausforming treatment

After having applied deformation, the signal intensity is lower

isotropic

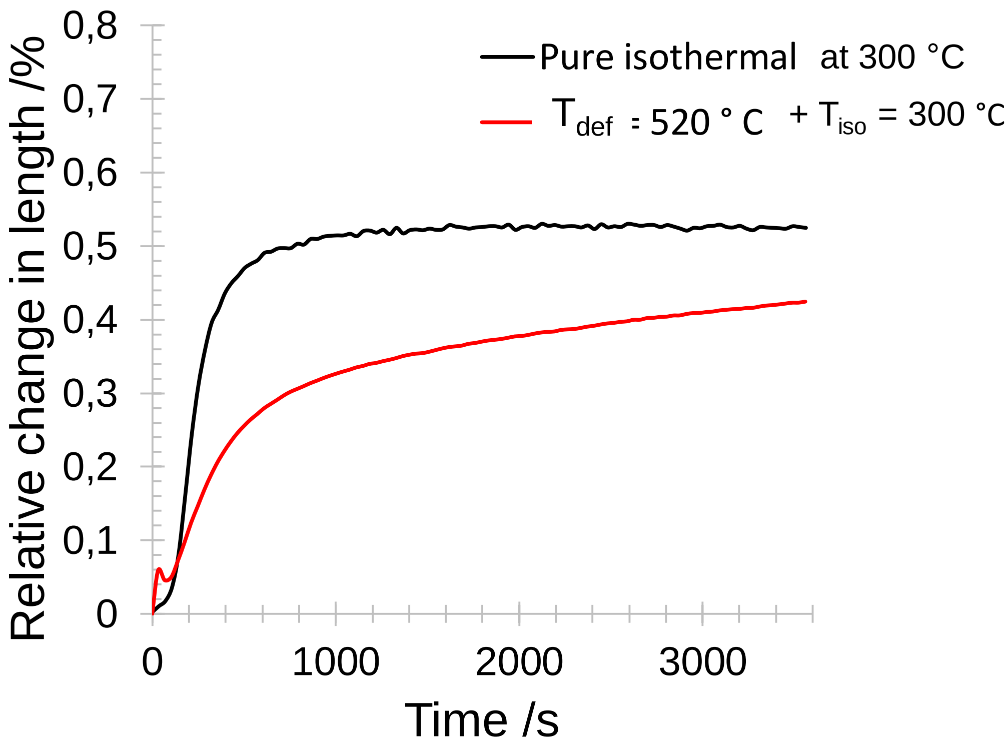

Transverse section

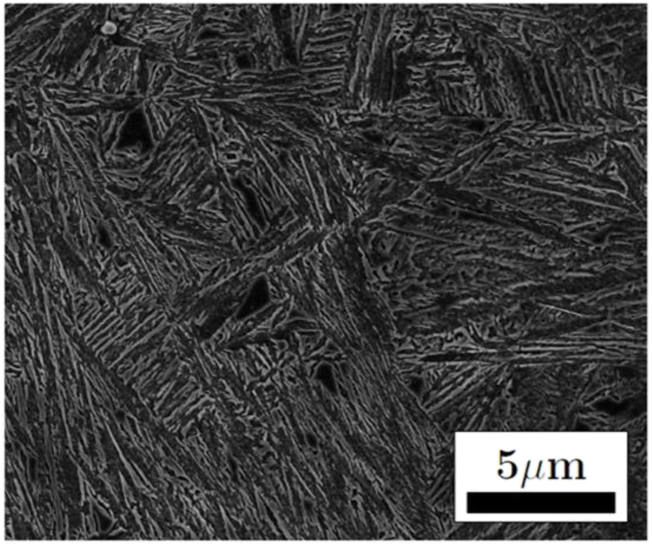

Longitudinal section

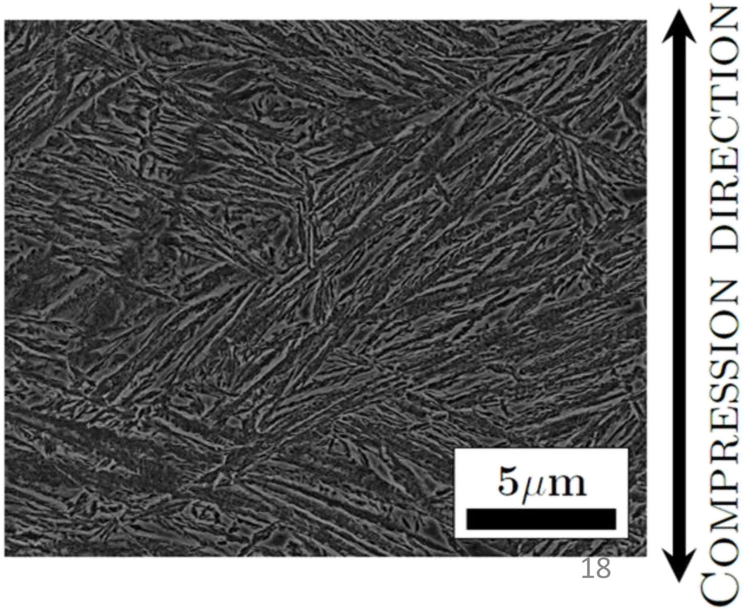

Results:

Ausforming treatments

After having applied deformation, the signal intensity is lower or even the signal becomes negative

anisotropic

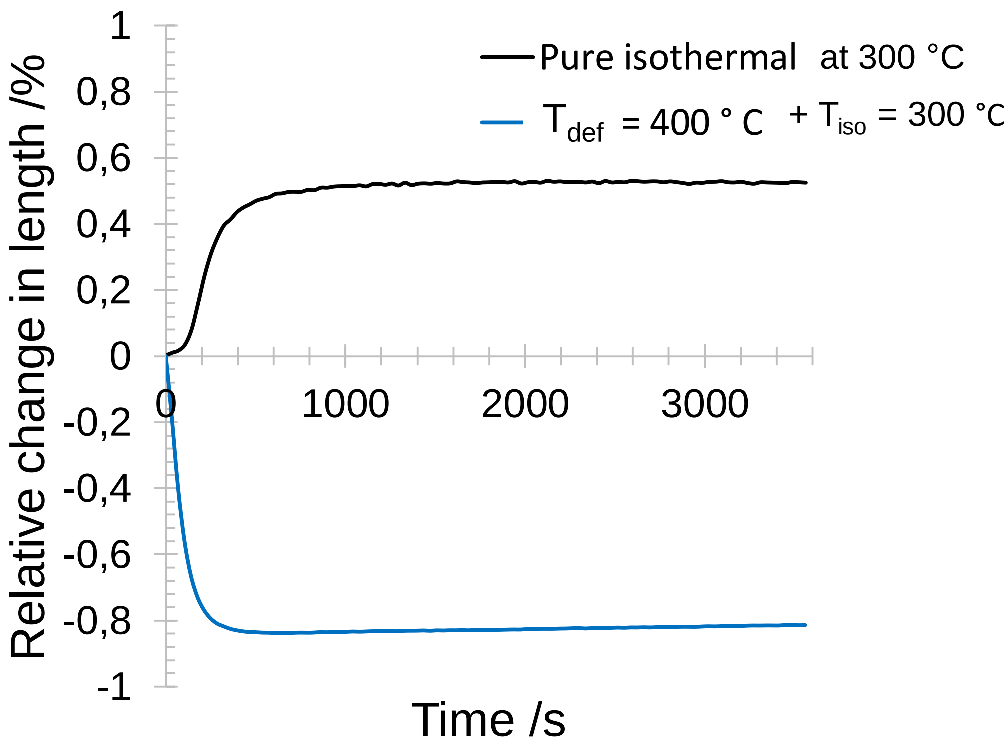

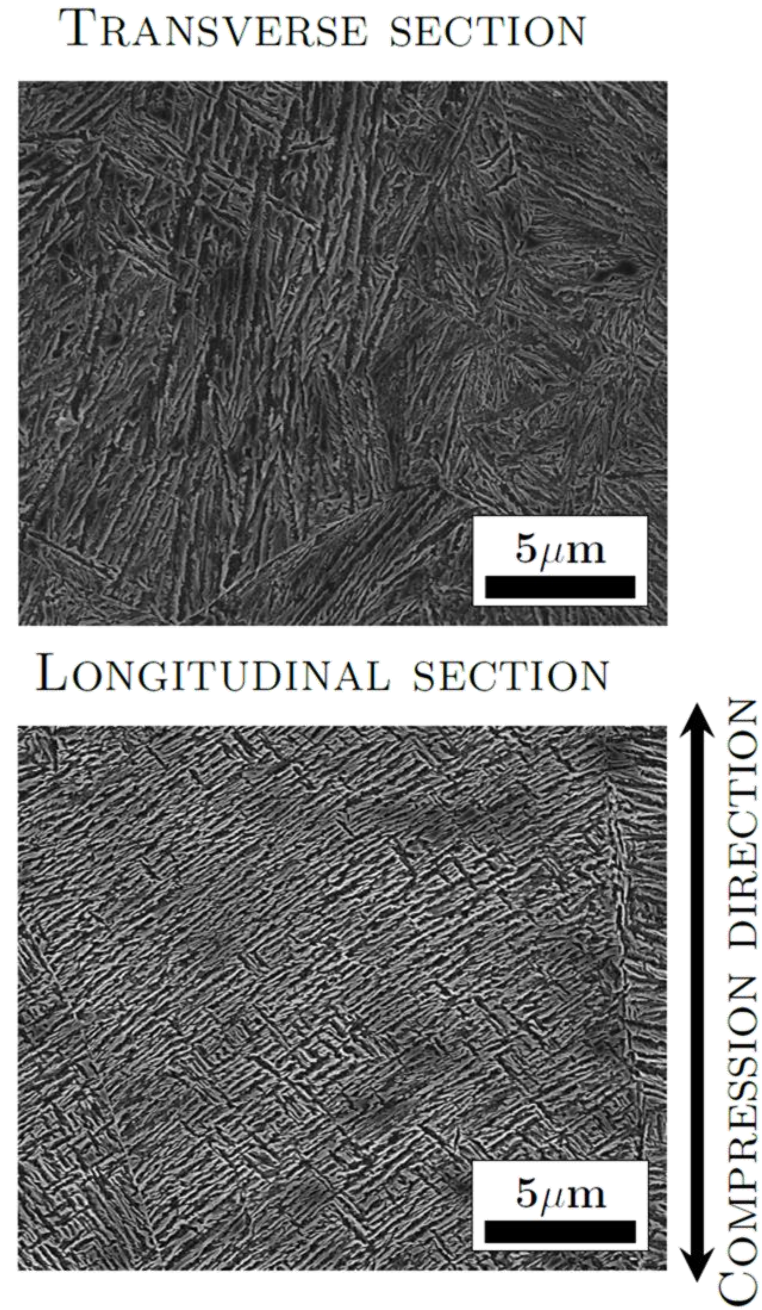

Results:
Ausforming treatments

After having applied deformation, the signal intensity is lower or even the signal becomes negative

anisotropic

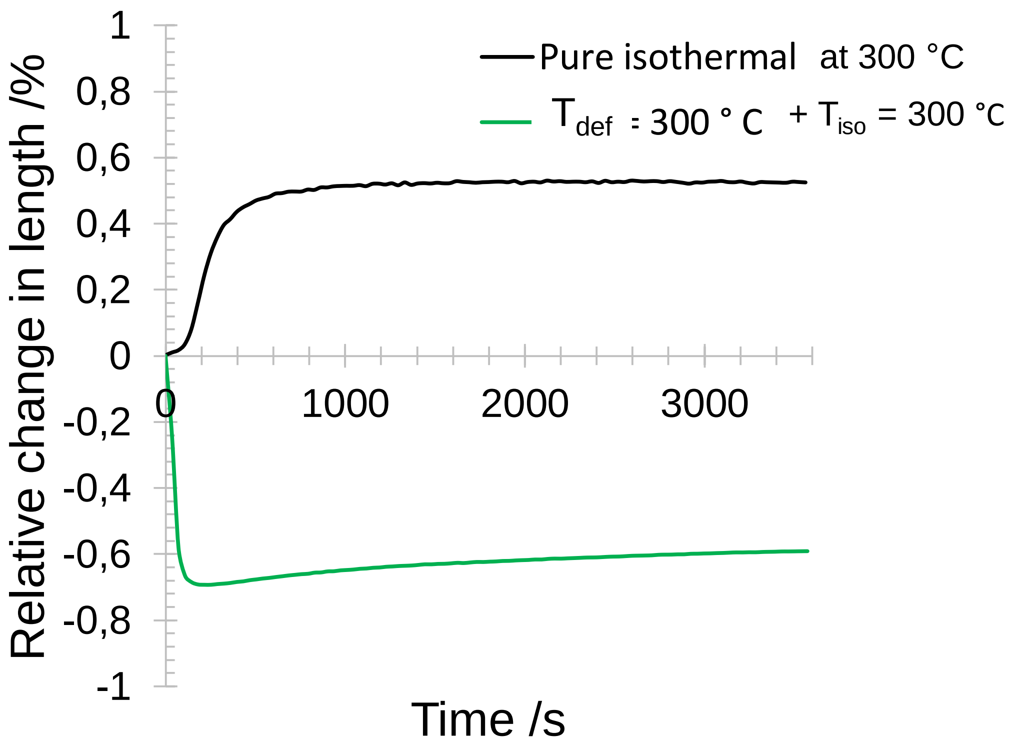

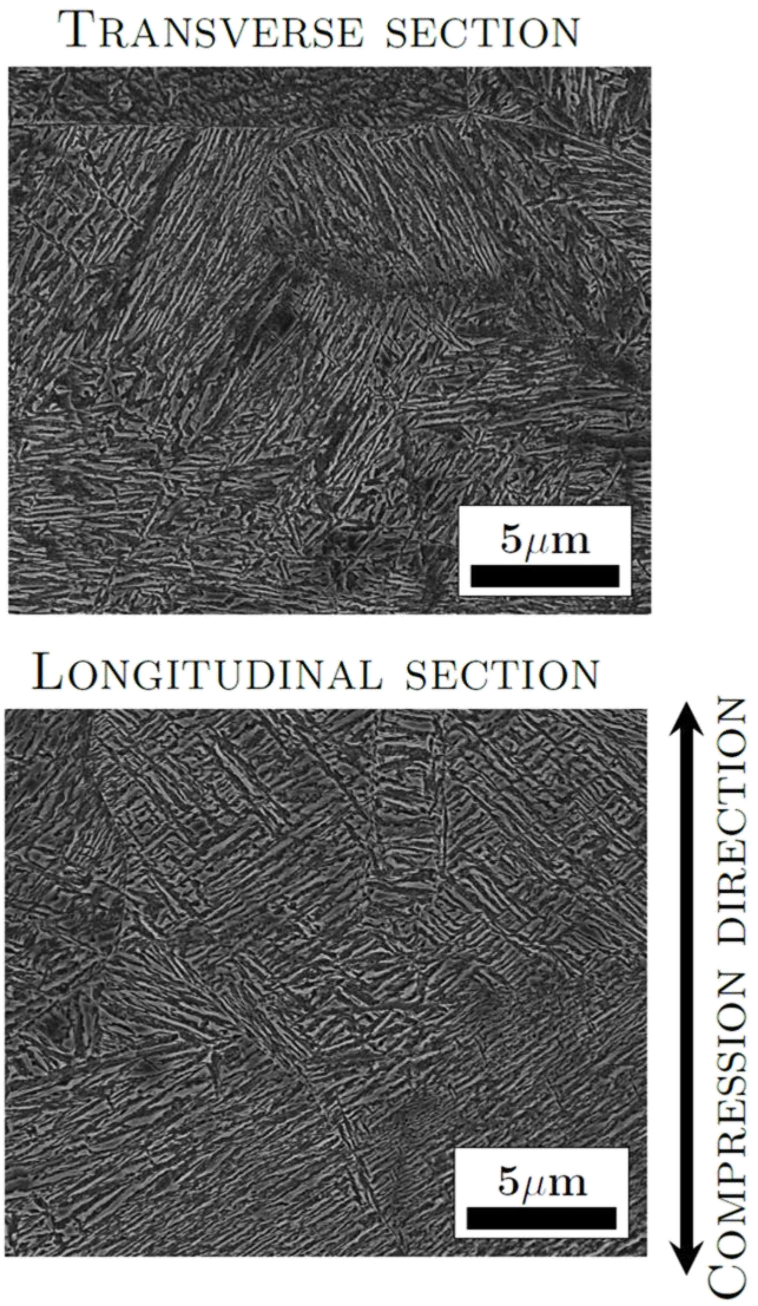

Results:

Ausforming treatments

T_{def} = 400 °C + T_{iso} = 300 °C

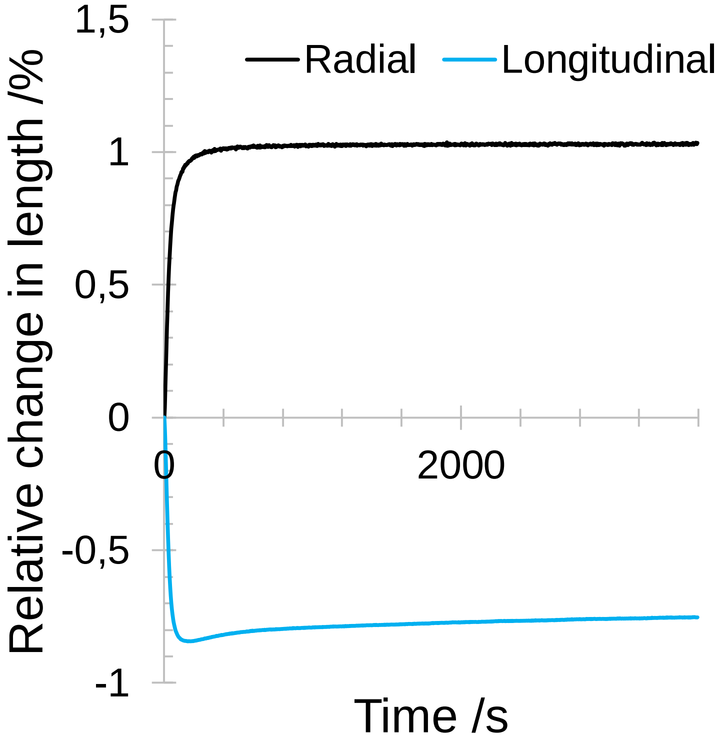

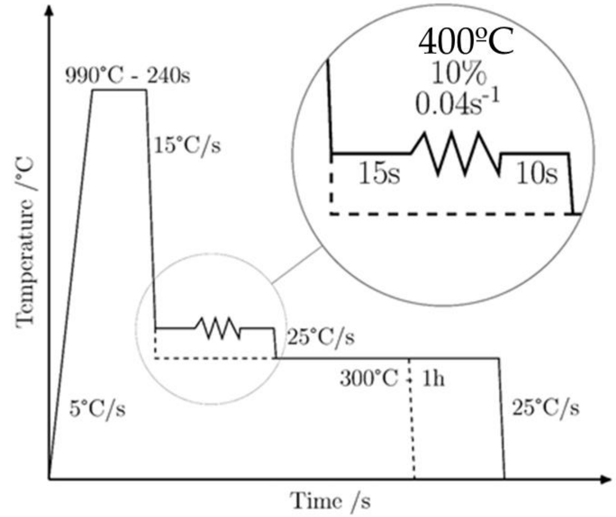

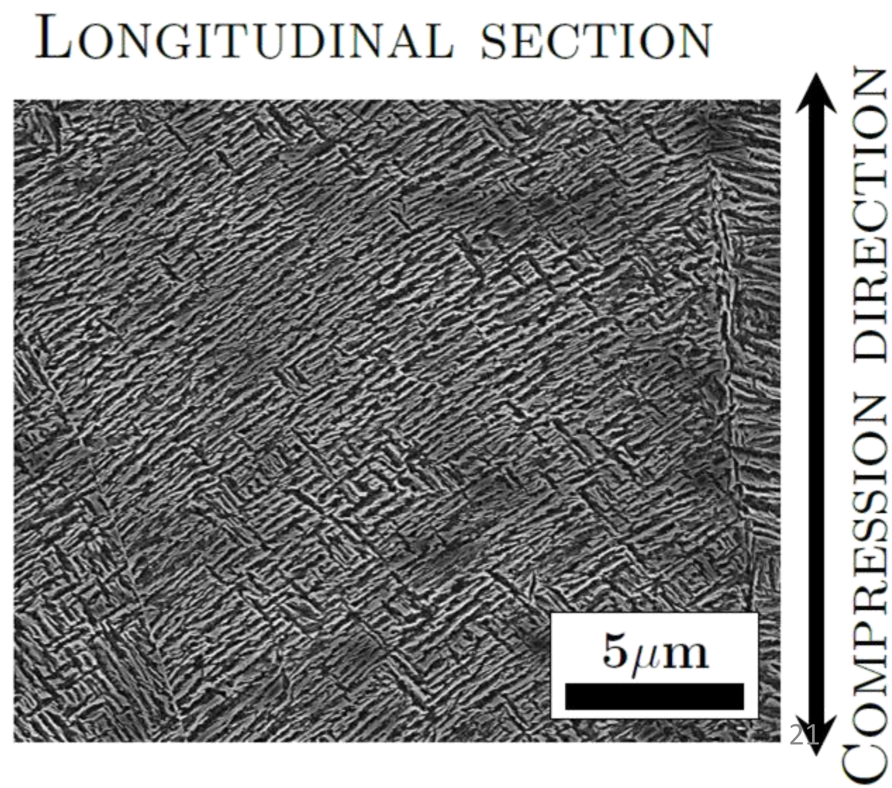

Results: crystallographic study - T_{def} = 400 °C + T_{iso} = 300 °C

The microstructures have being studied by EBSD, everything indicates that the microstructures are ordered because of variant selection.

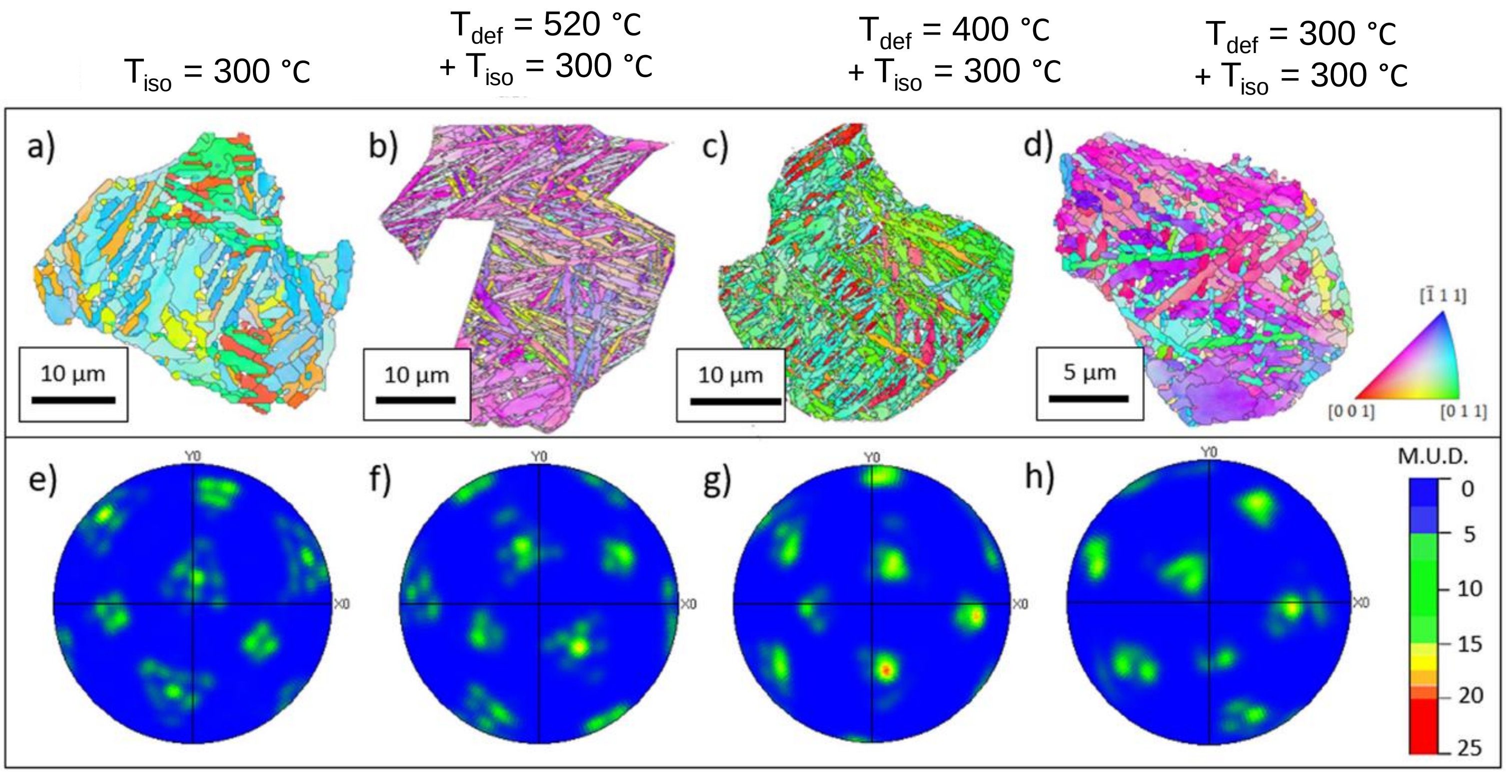

Results: Is the variant selection related to the negative longitudinal dilatometry signal? – T_{def} = 400 °C + T_{iso} = 300 °C

Microstructure → EBSD map (bainitic ferrite) → Reconstruction of Prior Austenite → Application of PTM

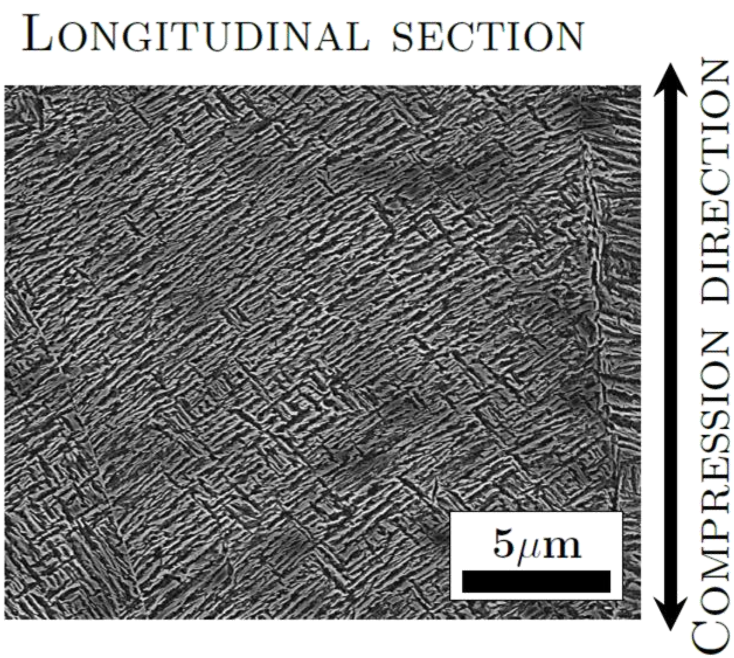

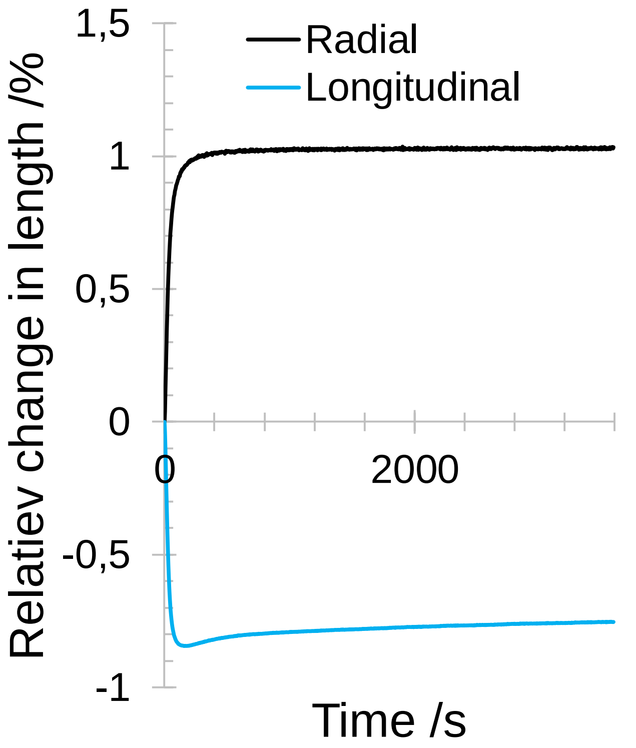

Results: Is the variant selection related to the negative longitudinal dilatometry signal? – T_{def} = 400 °C + T_{iso} = 300 °C

Microstructure → EBSD map (bainitic ferrite) → Reconstruction of Prior Austenite → Application of PTM

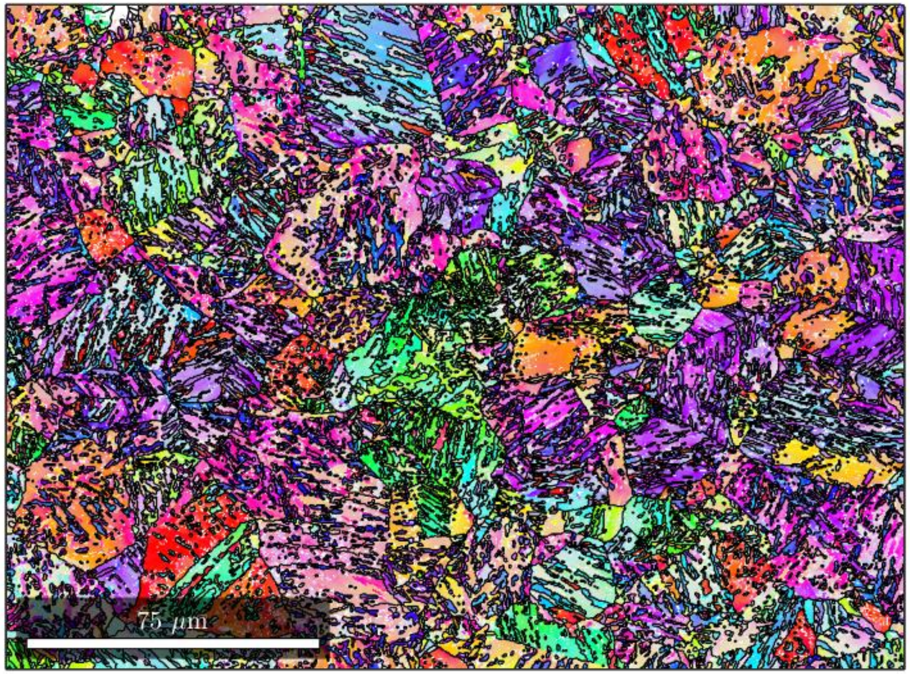

Ferrite

Results: Is the variant selection related to the negative longitudinal dilatometry signal? – T_{def} = 400 °C + T_{iso} = 300 °C

Microstructure → EBSD map (bainitic ferrite) → Reconstruction of Prior Austenite * → Application of PTM

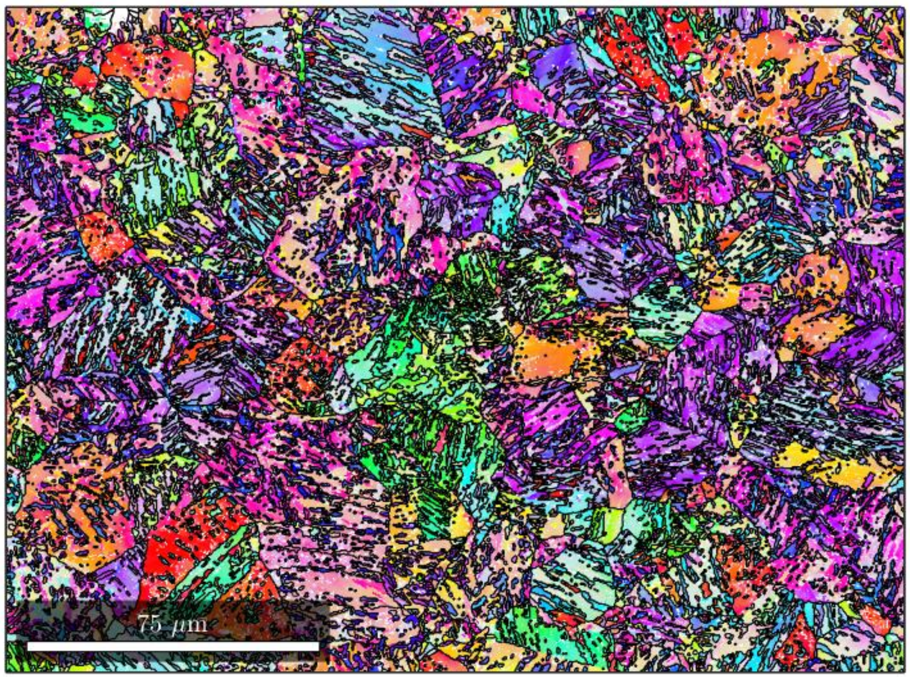

Ferrite

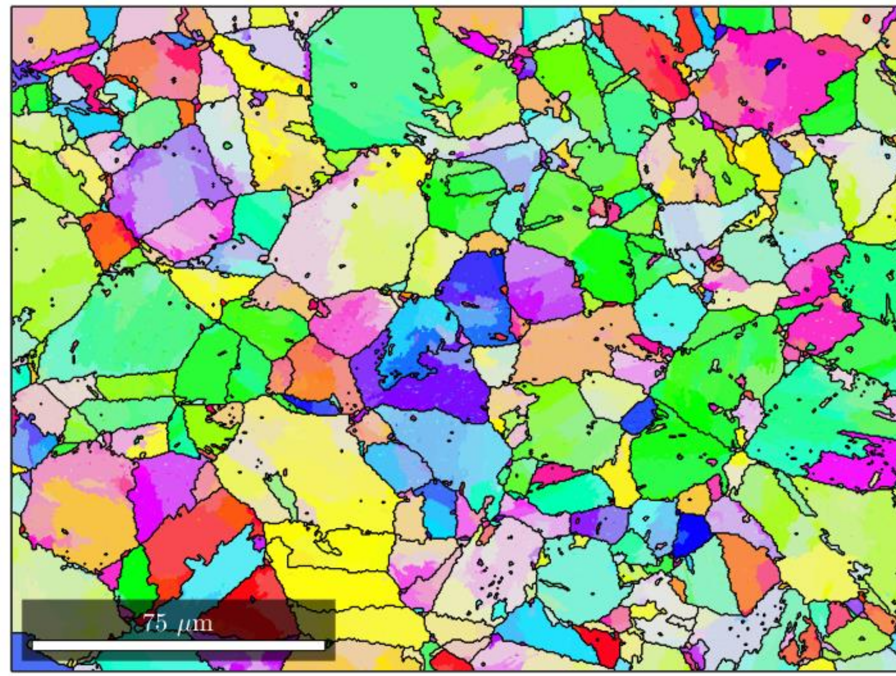

Austenite

* T. Nyyssönen, P. Peura, V.-T. Kuokkala, Crystallography, morphology, and martensite transformation of prior austenite in intercritically annealed high-aluminum steel, Metall. Mater. Trans. A, 49 (2018) 6426-6441.

Results: Is the variant selection related to the negative longitudinal dilatometry signal? – T_{def} = 400 °C + T_{iso} = 300 °C

Microstructure → EBSD map (bainitic ferrite) → Reconstruction of Prior Austenite → Application of PTM

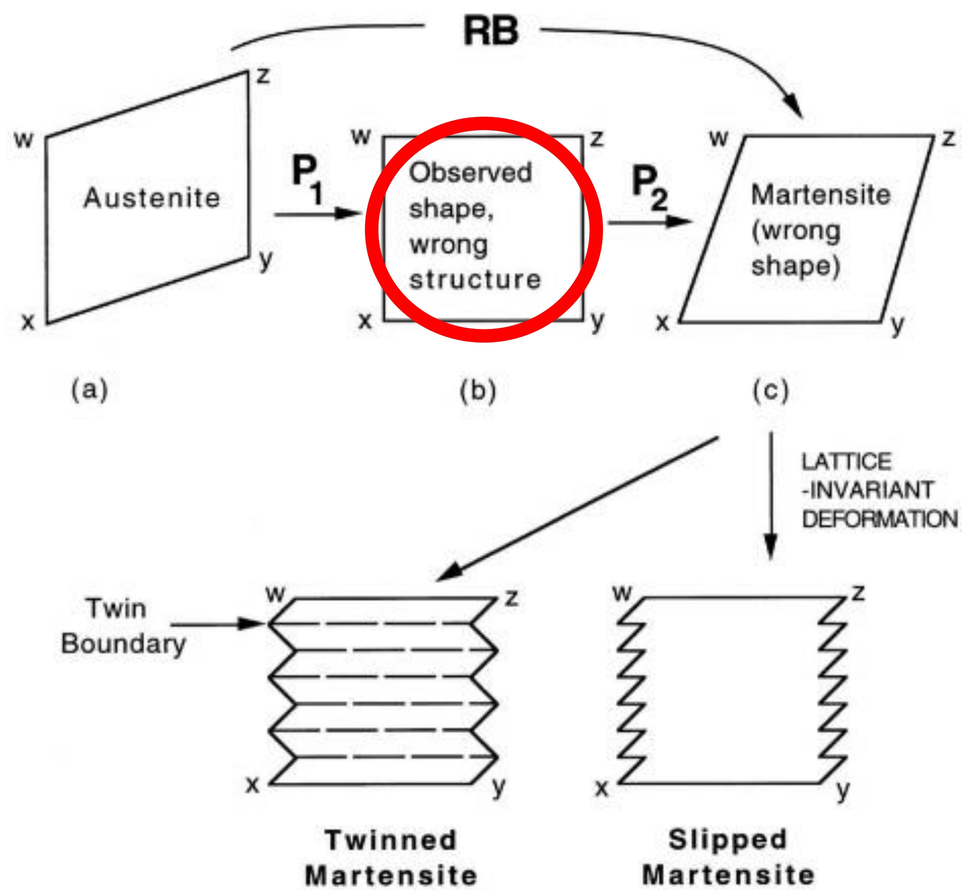

Results: Outcome for a theoretical random distribution

Changes in length for a theoretical random distribution (no variant selection)

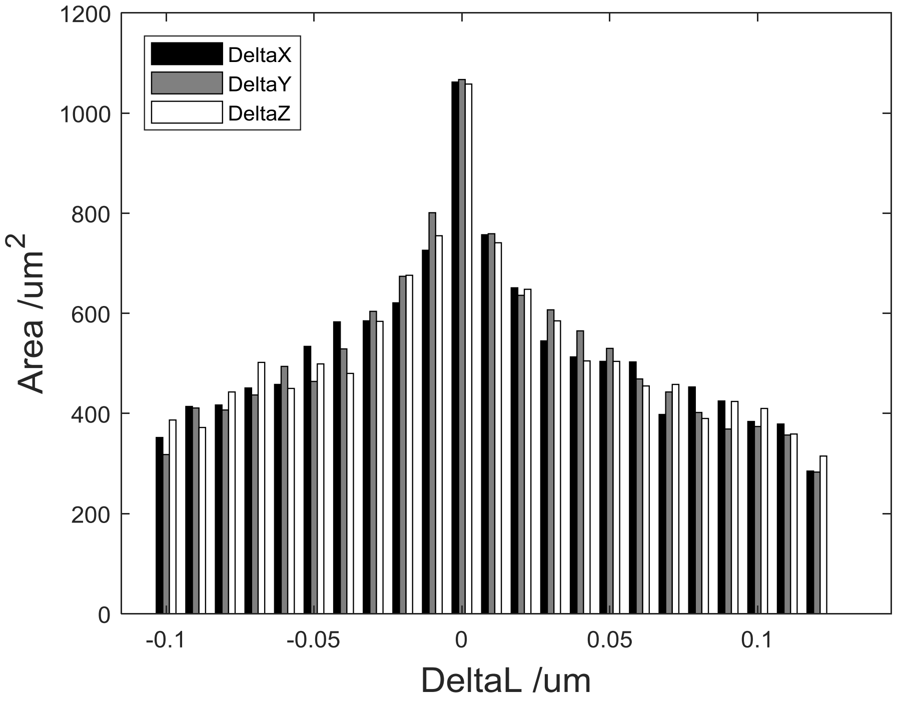

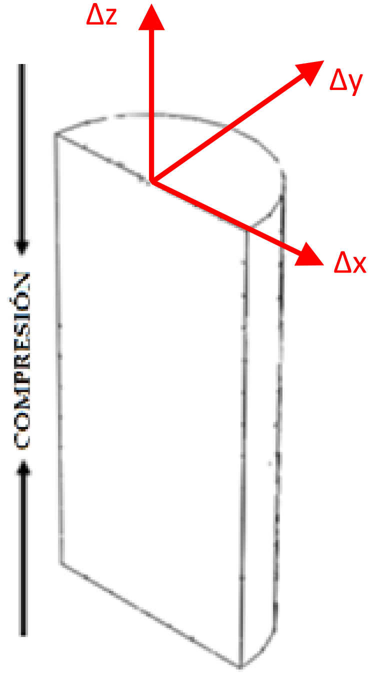

$\Delta y = \Delta x = \Delta r$
$\Delta z = \Delta L$

Results: Outcome for a theoretical random distribution

Changes in length for a theoretical random distribution (no variant selection)

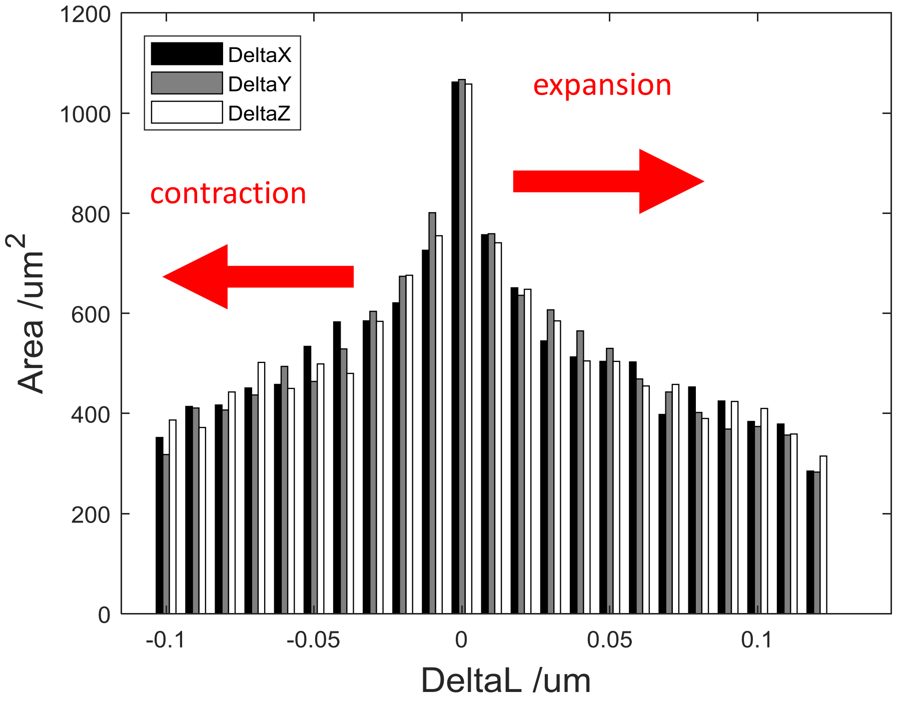

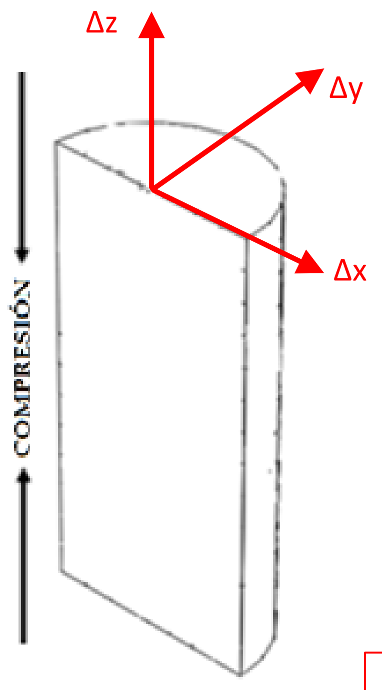

Δy=Δx=Δr
Δz=ΔL

Δr=ΔL>0

Results: Outcome obtained from the experimental EBSD data - T_{def} = 400 °C + T_{iso} = 300 °C

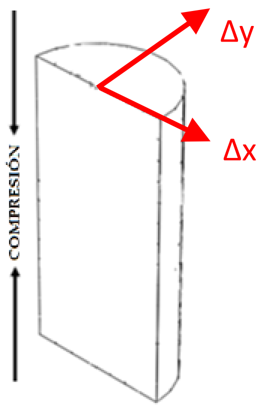

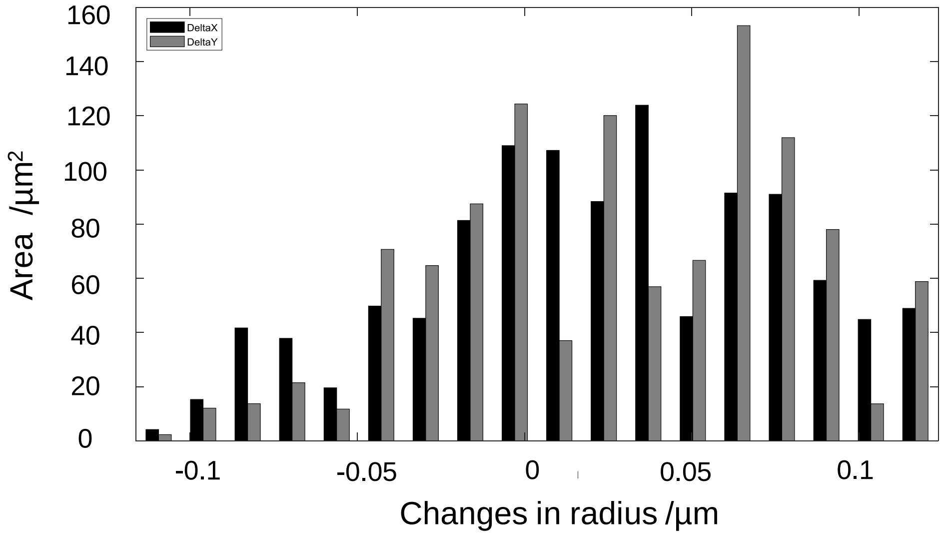

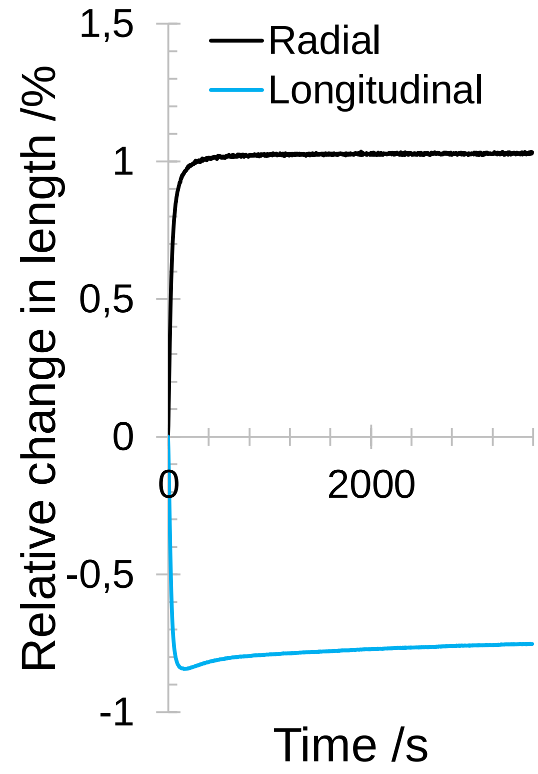

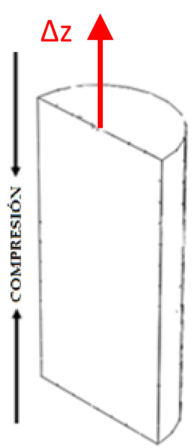

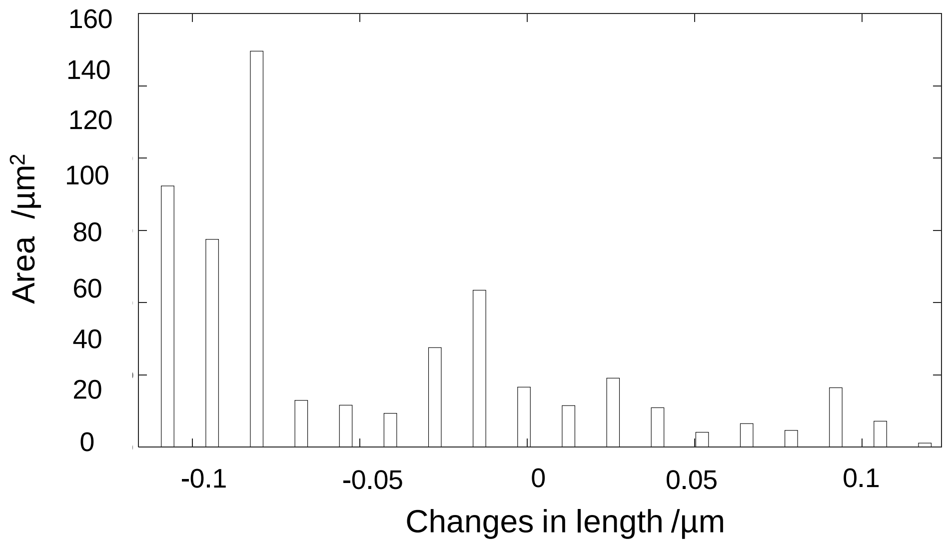

Conclusions

→ LT Ausforming treatments lead to anisotropic microstructures, highly ordered, whereas MT ausforming and pure isothermal treatments do not present such an anisotropy.

→ LT ausforming provokes that some crystallographic variants are selected during the bainitic transformation, whereas such phenomena do not occur for MT ausforming and pure isothermal treatments.

→ The negative dilatometric signals can be explained crystallographically by applying the Phenomenological Theory of Martensite.

Publications on the topic

Materials Characterization 145 (2018) 371–380

ELSEVIER

Contents lists available at ScienceDirect

Materials Characterization

journal homepage: www.elsevier.com/locate/matchar

MATERIALS CHARACTERIZATION

Check for updates

Effect of ausforming on the anisotropy of low temperature bainitic transformation☆

Adriana Eres-Castellanos[a], Lucia Morales-Rivas[b], Andreas Latz[c], Francisca G. Caballero[a], Carlos Garcia-Mateo[a,*]

[a] National Center for Metallugical Research (CENIM-CSIC), Avda. Gregorio del Amo 8, Madrid 28040, Spain
[b] Technische Universität Kaiserslautern (TUK), Materials Testing, Gottlieb-Daimler-Str., 67663 Kaiserslautern, Germany
[c] thyssenkrupp Steel Europe AG, Technology & Innovation, Modelling and Simulation, Kaiser-Wilhelm-Straße 100, 47166 Duisburg, Germany

A. Eres-Castellanos, F.G. Caballero, C. Garcia-Mateo and L. Morales-Rivas. *Effect of ausforming on the final texture of bainitic microstructures.* (submitted)

Future work

- Study of evolution of texture during the deformation step and the isothermal holding by synchrotron (PETRA III)
- Study of the mechanisms that lead the transformations (stress/strain assisted?) by EBSD and TEM
- Study of possible deformation induced transformations during the compression step by dilatometry and SEM
- Study of the effect of ausforming on the final mechanical properties by tensile tests along longitudinal and transverse directions

Thank you all !!

Adriana Eres-Castellanos
aeres@cenim.csic.es